

Temperature-dependent optical constants and birefringence of nematic liquid crystal 5CB in the terahertz frequency range

Ru-Pin Pan, Cho-Fan Hsieh, Ci-Ling Pan, and Chao-Yuan Chen

Citation: *Journal of Applied Physics* **103**, 093523 (2008); doi: 10.1063/1.2913347

View online: <http://dx.doi.org/10.1063/1.2913347>

View Table of Contents: <http://scitation.aip.org/content/aip/journal/jap/103/9?ver=pdfcov>

Published by the [AIP Publishing](#)

Articles you may be interested in

[Terahertz optical constants of ytterbium-doped yttrium aluminum garnet crystals](#)

J. Appl. Phys. **99**, 093110 (2006); 10.1063/1.2195891

[Calculation of the birefringences of nematic liquid crystals at optical and infrared wavelengths](#)

J. Chem. Phys. **123**, 134904 (2005); 10.1063/1.2035083

[High-efficiency optical transfer of torque to a nematic liquid crystal droplet](#)

Appl. Phys. Lett. **82**, 4657 (2003); 10.1063/1.1588366

[Wide nematic range alkenyl diphenyldiacetylene liquid crystals](#)

Appl. Phys. Lett. **77**, 957 (2000); 10.1063/1.1288600

[High birefringence and wide nematic range bis-tolane liquid crystals](#)

Appl. Phys. Lett. **74**, 344 (1999); 10.1063/1.123066



Re-register for Table of Content Alerts

Create a profile.



Sign up today!



Temperature-dependent optical constants and birefringence of nematic liquid crystal 5CB in the terahertz frequency range

Ru-Pin Pan,^{1,a)} Cho-Fan Hsieh,¹ Ci-Ling Pan,² and Chao-Yuan Chen²

¹Department of Electrophysics, National Chiao Tung University, 1001 Ta Hsueh Road, Hsinchu, Taiwan 30010

²Institute of Electro-optical Engineering and Department of Photonics, National Chiao Tung University, 1001 Ta Hsueh Road, Hsinchu, Taiwan 30010

(Received 11 October 2007; accepted 2 March 2008; published online 8 May 2008)

We have measured the frequency dependence and temperature dependence of the optical constants of a liquid crystal 4'-*n*-pentyl-4-cyanobiphenyl (5CB) in both nematic and isotropic phases by using terahertz time-domain spectroscopy. The extinction coefficient of 5CB is less than 0.02 and without sharp absorption features in the frequency range of 0.2–1.0 THz. The extraordinary and ordinary indices of refraction at 25 °C are around 1.77 and 1.58, respectively, giving rise to a birefringence of 0.20 ± 0.02 in this frequency range. The temperature-dependent order parameter extracted from birefringence agrees with the results from the visible region quite well. © 2008 American Institute of Physics. [DOI: 10.1063/1.2913347]

I. INTRODUCTION

Knowledge of the frequency dependence, temperature dependence, and the magnitude of the extraordinary and ordinary refractive indices, n_e and n_o , as well as the birefringence ($\Delta n = n_e - n_o$) of liquid crystals (LCs), is crucial for both fundamental understanding and practical applications of LCs. Many groups have investigated the birefringence of LCs in the visible.^{1–5} In the infrared, the refractive indices and other optical properties of some LCs have also been reported.^{6–9} In the millimeter wave range, Lim *et al.*¹⁰ showed that many LCs have comparatively large birefringence with approximate values in the range of 0.1–0.18 at 30 GHz. Further, the birefringence of these LCs varied only slightly in the 15–94 GHz range. Based on this, LC-based waveguidelike or microstriplike phase shifters in millimeter wave regions have been demonstrated.^{10–12}

In the far-infrared (submillimeter wave) or terahertz frequency range, the absorption spectra ($6\text{--}200\text{ cm}^{-1}$) of typical LC compounds *N*-(*p*-methoxybenzylidene)-*p*-*n*-butylaniline (MBBA) and 4,4'-azoxydianisole (PAA) were studied over two decades ago.^{13,14} More recently, the refractive indices and transmission losses for some nematic LCs, including 4'-*n*-pentyl-4-cyanobiphenyl (5CB), were measured by Nose *et al.*¹⁵ at three discrete wavelengths (118, 215, and 435 μm). The refractive indices of 5CB for ordinary (n_o) and extraordinary rays (n_e) in the submillimeter wave region were found to be slightly larger than those in the visible range. By employing terahertz time-domain spectroscopy (TDS),¹⁶ we have shown that the terahertz (0.2–1.0 THz) birefringence of 5CB is in the range of 0.15–0.21, while that of *trans*-4'-Pentylcyclohexyl-benzonitrile (PCH5) is from 0.01 to 0.08 at room temperature.^{17–19} About the same values of birefringence were reported in the LC mixture, E7 (by Merck)²⁰ and a LC polymer.²¹ High-frequency dielectric relaxation of LCs was revealed through a terahertz

time-domain spectroscopic studies of LC colloids.²² Strong terahertz dichroism of MBBA on rubbed substrate was observed.²³ The isotropic liquid, LC and crystal phases of the bent-core LC P-8-PIMB were found to be clearly distinguished by their terahertz spectra.²⁴

Here, we report our improved and more accurate measurements of the complex optical constants of 5CB at 25 °C. Our previous data show a slow and monotonic increasing trend with frequency for both n_e and n_o in the 0.3–0.8 THz range. Specifically, n_e increases from 1.7 to 1.96, while n_o varies from 1.55 to 1.75. This is unexpected and its origin is identified in this work. We confirm that the complex optical constants of 5CB do not exhibit appreciable frequency dependence from 0.2 to 1.0 THz. The temperature dependence of the complex optical constant of 5CB and the order parameter of 5CB in the far infrared are also reported.

II. EXPERIMENTAL METHODS

Two types of cells, a reference cell and a homogeneously aligned LC cell, were prepared in this work. These are schematically shown in Fig. 1. The reference cell was constructed by two fused silica windows with nominal thickness of 3.0 mm each and in contact with each other. For the LC cell, a nematic LC layer (5CB, Merck) was sandwiched between two fused silica windows as substrates. The thickness of the LC layer was controlled with the Mylar spacers and mea-

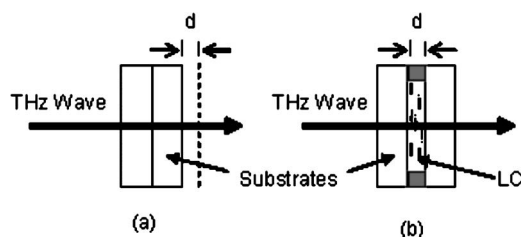


FIG. 1. Sketches of (a) the reference cell and (b) the LC cell. The substrates are fused silica and the alignment of LC cell is homogeneous.

^{a)}Electronic mail: rpchao@mail.nctu.edu.tw.

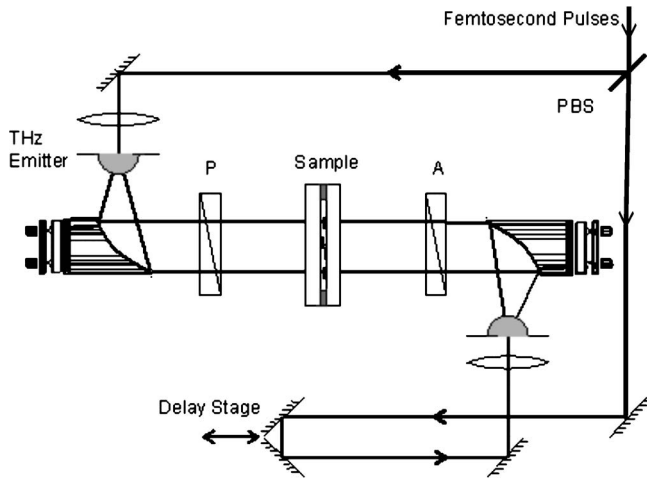


FIG. 2. Schematic of the terahertz-TDS. PBS: polarization beam splitter. *P* and *A*: terahertz polarizer and analyzer, respectively.

sured by subtracting the substrates thicknesses from the total cell thickness. The LC layer thickness in this work is $260 \pm 3 \mu\text{m}$ unless otherwise noted. Homogeneous alignment was achieved by coating polyimide on inner surfaces of the substrates followed by mechanical rubbing.²⁵ The measured pretilt angle was about 2° .²⁶ The temperature of the LC cell can be varied and controlled to 0.05°C . The substrates were chosen such that the total thicknesses of the two substrates for these two cells are equal with an accuracy of $2 \mu\text{m}$.

An antenna-based terahertz-TDS system with a collimated beam at the sample position²⁷ had been used. A schematic of the terahertz-TDS system is shown in Fig. 2. Terahertz pulses, generated by femtosecond-laser-excited dipolelike antenna fabricated on low-temperature-grown GaAs, were collimated by an off-axis paraboloidal mirror and propagated through the sample at normally incidence. A pair of parallel wire-grid polarizers, before and after the sample, was employed in order to ensure the polarization state of the terahertz wave. The terahertz fields of *e* ray and *o* ray are parallel and perpendicular to the aligned direction of LC cell, respectively. The transmitted terahertz pulses were focused on another dipolelike antenna gated by time-delayed probe pulses and oriented to detect terahertz waves polarized parallel to the incident terahertz wave polarization. The beam size of the terahertz wave through the sample is about 0.8 cm in diameter.

There are several absorption lines of water vapor in the frequency range of $0.2\text{--}1.5 \text{ THz}$.²⁸ Our terahertz time-domain spectrometer can be purged with nitrogen and maintained at a relative humidity of $(3.0 \pm 0.5)\%$. The terahertz time-domain signals and the frequency spectra before and after purging are shown in Figs. 3(a) and 3(b), respectively.

III. DETERMINATION OF OPTICAL CONSTANTS

We assume that the terahertz signal is a plane wave passing through the cell at normal incidence. The electric field of the terahertz wave transmitted through the reference cell at an angular frequency ω can then be written as

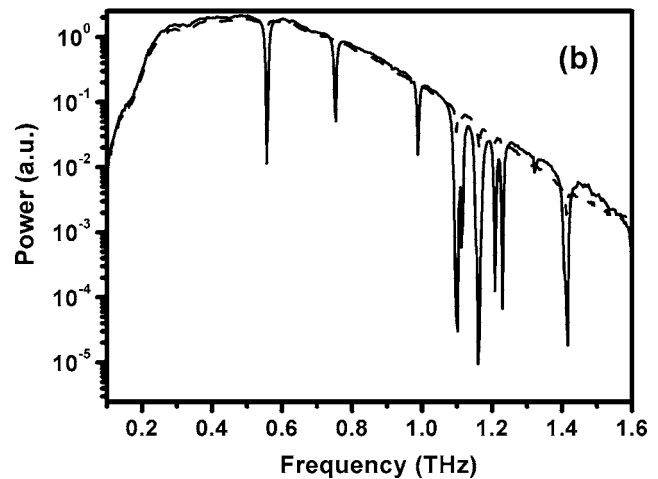
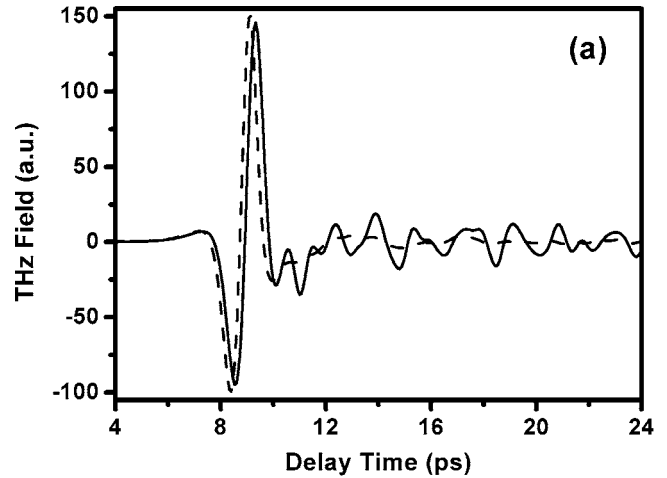


FIG. 3. (a) Temporal profiles of the terahertz signals before (solid line) and after (dash line) purging. (b) The power spectra of the terahertz signals before (solid line) and after (dash line) purging. Several absorption lines of water vapor appear before purging. The relative humidities before and after purging are 53% and 3% , respectively.

$$E_{\text{ref}}(\omega) = E_0(\omega) \eta(\omega) P_{\text{air}}(\omega, d), \quad (1)$$

where $E_0(\omega)$ is the electric field of the incident terahertz wave. The parameter $\eta(\omega)$ takes into account the Fabry-Pérot effect due to the Fresnel reflection of the terahertz wave at the quartz-air interfaces and its propagation in fused silica. The propagation coefficient in air over a distance d is denoted by $P_{\text{air}}(\omega, d) = \exp[-i\tilde{n}_{\text{air}}\omega d/c]$, where \tilde{n}_{air} is the complex refractive index of air and the value of 1 is assumed in this work. The length d is chosen to be the same as that of the LC layer (see Fig. 1). Similarly, the electric field of the terahertz wave transmitted through the LC cell can be written as

$$E_{\text{LC}}(\omega) = E_0(\omega) \eta(\omega) T_{q\text{-LC}}(\omega) P_{\text{LC}}(\omega, d) \times T_{\text{LC-q}}(\omega) \text{FP}_{\text{LC}}(\omega, d), \quad (2)$$

where $T_{q\text{-LC}}(\omega) = (2\tilde{n}_q)/(\tilde{n}_q + \tilde{n}_{\text{LC}})$ and $T_{\text{LC-q}}(\omega) = (2\tilde{n}_{\text{LC}})/(\tilde{n}_{\text{LC}} + \tilde{n}_q)$ are the transmission coefficients of the quartz-LC and LC-quartz interfaces, respectively; $P_{\text{LC}}(\omega, d) = \exp[-i\tilde{n}_{\text{LC}}\omega d/c]$ and $\text{FP}_{\text{LC}}(\omega, d)$ are the propagation and Fabry-Pérot coefficients in the LC layer with a thickness of

d , respectively. The coefficient $\eta(\omega)$ for the LC cell is the same as that for the reference cell because of the thicknesses of the fused silica windows used are the same (tolerance $< 2 \mu\text{m}$). The complex transmittance $T(\omega)$ of the LC layer can then be obtained by dividing $E_{\text{LC}}(\omega)$ by $E_{\text{ref}}(\omega)$

$$T(\omega) = \frac{4\tilde{n}_{\text{LC}}\tilde{n}_q}{(\tilde{n}_{\text{LC}} + \tilde{n}_q)^2} \exp\left[-i(\tilde{n}_{\text{LC}} - \tilde{n}_{\text{air}})\frac{\omega d}{c}\right] \text{FP}_{\text{LC}}(\omega, d), \quad (3)$$

where \tilde{n}_q is the complex refractive index of fused silica and \tilde{n}_{LC} is either the ordinary index ($\tilde{n}_o = n_o - i\kappa_o$) or extraordinary index ($\tilde{n}_e = n_e - i\kappa_e$) of the LC layer.

For optically thick samples, the echoes of terahertz waves from the multiple reflections of the sample are temporally well separated from the main signal. These can be easily removed without affecting the accuracies of the measurements. Thus, we can set $\text{FP}_{\text{LC}}(\omega, d) = 1$ in Eq. (3).²⁹ On the other hand, if the sample is optically thin, the Fabry–Pérot effect need be considered. Instead of solving $T(\omega) - T_{\text{meas}}(\omega) = 0$, in which $T(\omega)$ and $T_{\text{meas}}(\omega)$ are the calculated and measured complex transmission coefficients, respectively, the Newton–Raphson method was used for extracting the optical constants.³⁰ We define an error function

$$\delta(n, \kappa) = \delta\rho^2 + \delta\varphi^2,$$

where

$$\delta\rho = \ln[|T(\omega)|] - \ln[|T_{\text{meas}}(\omega)|], \quad (4a)$$

$$\delta\varphi = \arg[T(\omega)] - \arg[T_{\text{meas}}(\omega)], \quad (4b)$$

where $T(\omega)$ and $T_{\text{meas}}(\omega)$ are the calculated, i.e., [Eq. (3)] and experimentally measured complex transmission coefficients, respectively. As defined above, the error function $\delta(n, \kappa)$ can be easily calculated with a given trial set of (n, κ) . Approximate values of n and κ were obtained by setting $\text{FP}(\omega) = 1$. In Eq. (3) and then this set was used as the initial trial values. After minimizing this error function with respect to (n, κ) , the optical constants n and κ are determined for any angular frequency ω .

IV. RESULTS AND DISCUSSIONS

A. Complex optical constants

Figure 4 shows an example of the measured time domain signals of terahertz waves that pass through the reference cell and LC cell at 25 °C for e ray and o ray. The time delay of signal passing through the LC cell with respect to that of the reference signal is evident. A relatively small signal, which is the reflection of terahertz wave from the quartz-LC interface, following the main terahertz pulse and about 10 ps behind is also observable. The main (first) terahertz signal becomes zero before this reflective signal arrives. In the following analysis, we have thus cut off the time-domain signal right before this reflective signal. The amplitude and the phase spectra of the terahertz wave passing through the LC cell and reference cell are obtained by applying a fast Fourier trans-

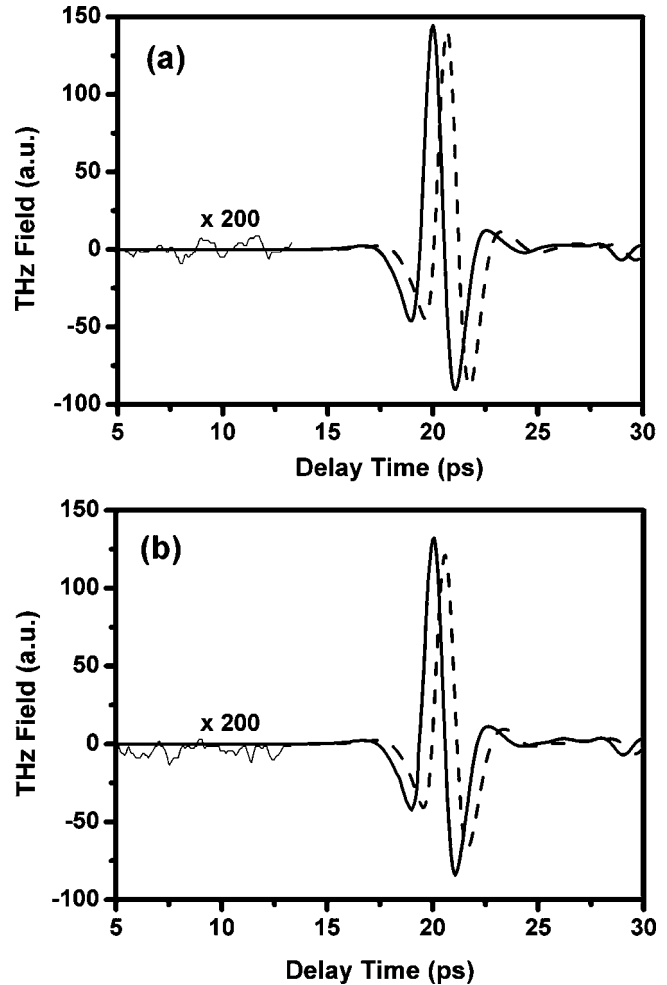


FIG. 4. Transmitted terahertz signals through the reference (solid line) and LC cells (dashed line) for (a) e ray and (b) o ray at 25 °C. The noise, magnified by two hundred times, is also shown as the thin solid lines.

form (FFT) to the time-domain waveforms. The optical constants of the LC are then determined using the procedure described in the previous section.

The real part and imaginary part of the optical constants of 5CB at 25 °C are shown as a function of frequency in Fig. 5. The filled circles and the open circles are the extraordinary and ordinary indices, n_e , n_o , respectively. The real parts of the indices show clear anisotropy, with $n_e = 1.77$ and $n_o = 1.58$, giving rise to a birefringence of 0.20 ± 0.02 . We note that $n_e = 1.706$ and $n_o = 1.529$ in the visible.³¹ The imaginary part of the refractive index of 5CB is smaller than 0.02 in the frequency range from 0.2 to 1.0 THz. It does not exhibit appreciable anisotropy.

It could be argued that the LC layer, 260 μm in thickness, is relatively thin compared to the wavelength of terahertz waves, consequently affecting the accuracies of the extracted optical constants. To check, we also measured the optical constants of a thicker LC layer with a thickness of 2.0 mm. This experiment was carried out at 38 °C where 5CB is in its isotropic phase. The data points are also shown in Fig. 5 as crosses. As expected, the real indices of 5CB in isotropic phase fall between n_e and n_o and are given approximately by $\sim(2n_o + n_e)/3$.³² The imaginary indices of 5CB in isotropic

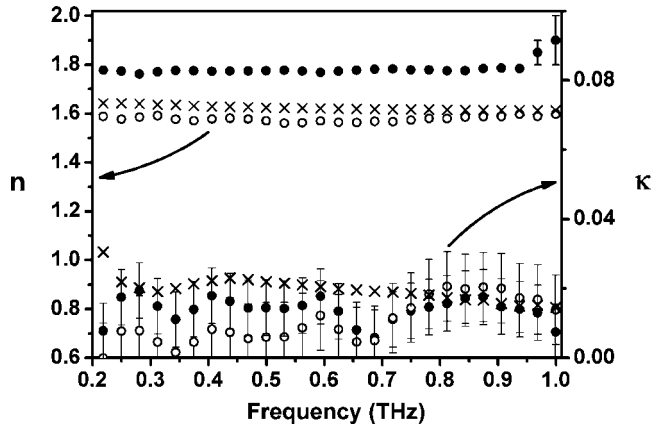


FIG. 5. The optical constants of 5CB, n and κ , are plotted as functions of frequency. The solid circles and the open circles are the extraordinary and ordinary indices at 25 °C, respectively. The crosses are the values of optical constants of 5CB in the isotropic phase at 38 °C. Error bars are indicated, unless they are smaller than the sizes of the symbols.

phase, on the other hand, is ~ 0.02 . No absorption features are observed in this frequency range. The above experiments confirm the reliability of our data.

B. Temperature dependence

The temperature dependence of the real indices of 5CB at frequencies of 0.344, 0.500, 0.656, and 0.750 THz are shown in Fig. 6. The filled and open circles are experimental data for n_e and n_o , respectively. Following Brugioni *et al.*,³³ we fit the temperature dependence of the real part of the refractive indices with

$$n = A \times (B - T_R)^C, \quad (5)$$

where n is the refractive index and T_R is the reduced temperature defined as the difference between measured sample temperature and measured clearing point ($T - T_c$). The fitting parameters A , B , and C thus obtained are shown in Table I. The fitting curves are also shown in Fig. 6 as the dotted line with the measured data. Above the transition temperature, i.e., in isotropic phase, the experimental points are shown in Fig. 6 with stars. Below the transition temperature, the solid lines show the average indices $(2n_o + n_e)/3$ from the fitting results.

C. Birefringence and order parameter

The temperature-dependent birefringence of 5CB at the frequencies of 0.344, 0.500, 0.656, and 0.750 THz are plotted in Fig. 7, in which the solid curves are the fitting results by using

$$\Delta n(T) = D \left(1 - \frac{ET}{T_C} \right)^F,$$

where D , E , and F are the fitting parameters. The order parameter of 5CB can be extracted from the fitting parameters as

$$S = \left(1 - \frac{ET}{T_C} \right)^F.$$

We find that $E = 0.985 \pm 0.01$ and $F = 0.21 \pm 0.02$. This agrees well with the order parameter of 5CB measured in the visible, where $E = 0.98$ and $F = 0.22$.³⁴ Since the order parameter is not expected to change, we conclude that the birefringence we measured in the terahertz range is reasonable and reliable.

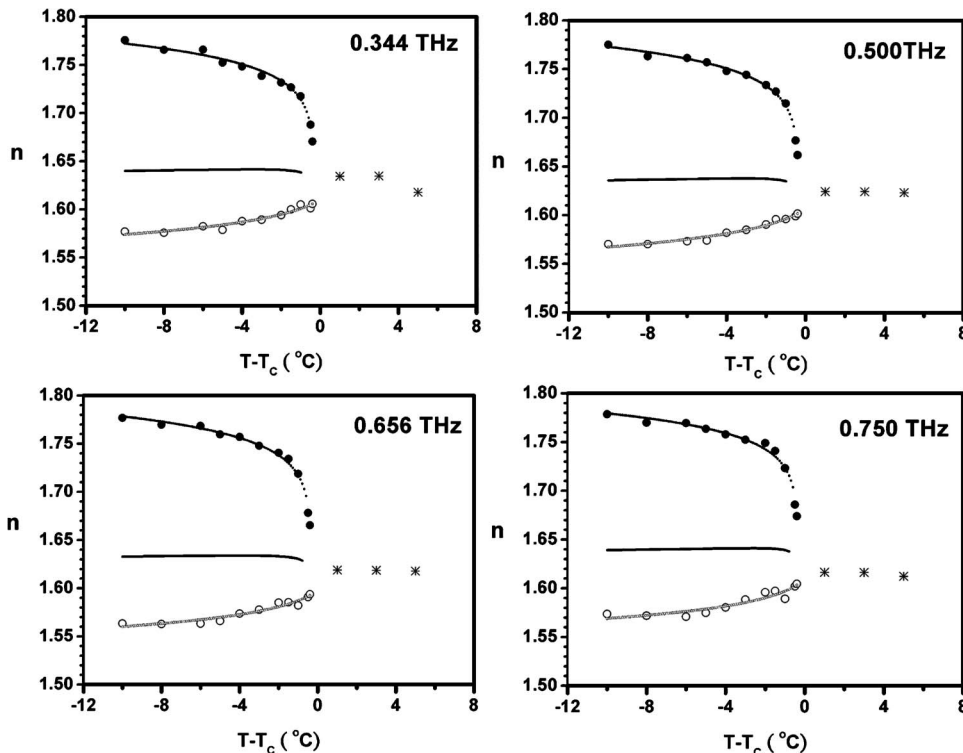


FIG. 6. Extraordinary and ordinary refractive indices of 5CB are plotted as functions of reduced temperature at frequencies of 0.344, 0.500, 0.656, and 0.750 THz. The solid and the open circles represent n_e and n_o , respectively. The stars are data for the refractive index of 5CB in the isotropic phase. The solid lines are the average index, $(2n_o + n_e)/3$ at temperatures below T_c .

TABLE I. The fitting parameters of Eq. (5) for frequencies from 0.219 to 0.937 THz. (A_o , B_o , C_o) and (A_e , B_e , C_e) are for n_o and n_e , respectively.

Frequency (THz)	A_o	B_o	C_o	A_e	B_e	C_e
0.219	1.706 159	-0.171 32	0.0145 33	1.621 996	0.484 098	-0.009 75
0.250	1.702 852	-0.156 19	0.0158 51	1.619 643	1.167 518	0.011 93
0.281	1.706 969	-0.269 22	0.0138 45	1.628 633	1.583 427	0.0114 44
0.312	1.715 861	-0.300 17	0.0129 51	1.632 112	1.527 217	0.0108 92
0.344	1.722 044	-0.30 57	0.0126 33	1.616 452	1.434 598	0.0109 21
0.375	1.722 979	-0.331 05	0.0123 97	1.610 879	1.686 762	0.0110 08
0.406	1.72 177	-0.343 56	0.0124 37	1.624 173	2.162 122	0.0121 89
0.437	1.719 191	-0.328 45	0.0127 78	1.632 175	2.294 422	0.0134 18
0.469	1.722 941	-0.342 57	0.0125 01	1.622 331	1.814 399	0.0119 93
0.500	1.721 391	-0.337 98	0.0129 82	1.612 512	1.39 94	0.0117 01
0.531	1.722 375	-0.348 91	0.0128 54	1.606 205	1.239 742	0.012 75
0.562	1.722 488	-0.346 96	0.0127 18	1.601 712	1.368 953	0.010 924
0.593	1.721 763	-0.352 48	0.0124 54	1.591 74	0.361 484	0.006 557
0.625	1.722 863	-0.356 94	0.0126 67	1.594 432	0.733 914	0.008 687
0.656	1.726 522	-0.34 29	0.0130 37	1.599 44	1.123 686	0.010 336
0.687	1.730 538	-0.333 06	0.0128 03	1.603 058	1.013 795	0.010 096
0.718	1.729 269	-0.343 55	0.0127 76	1.60 32	0.893 55	0.010 688
0.750	1.732 391	-0.350 94	0.0118 28	1.607 052	0.866 241	0.010 041
0.781	1.734 336	-0.359 63	0.0103 84	1.606 057	0.586 836	0.008 263
0.812	1.732 746	-0.366 79	0.009 6	1.602 829	0.292 01	0.007 685
0.843	1.733 756	-0.320 94	0.0105 42	1.605 666	0.169 034	0.006 281
0.875	1.734 888	-0.29 97	0.0110 57	1.597 293	-0.292 19	0.004 213
0.906	1.733 556	-0.284 55	0.0116 29	1.599 054	-0.130 45	0.005 06
0.937	1.728 894	-0.156 81	0.013 26	1.600 826	-0.286 45	0.003 455

D. Comparison to previous results

The refractive indices of 5CB in the terahertz frequency range were previously reported by the authors.^{17–19} We showed a slow and monotonic increasing trend with fre-

quency for both n_e and n_o in the 0.3–0.8 THz range. Specifically, n_e was found to increase from 1.7 to 1.96, while n_o varied from 1.55 to 1.75. Here, we present more accurate results, i.e., $n_e=1.77$ and $n_o=1.58$ at 25 °C giving rise to a

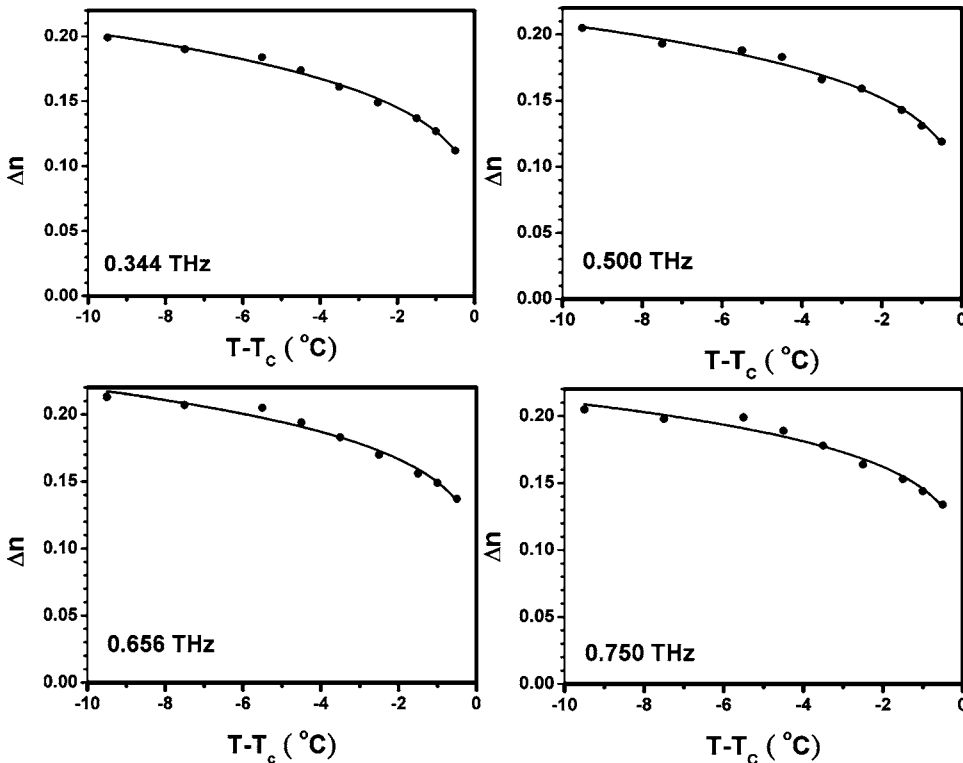


FIG. 7. Birefringence of 5CB measured at 0.344, 0.500, 0.656, and 0.750 THz are plotted as a function of reduced temperature. The curves are the fitting results.

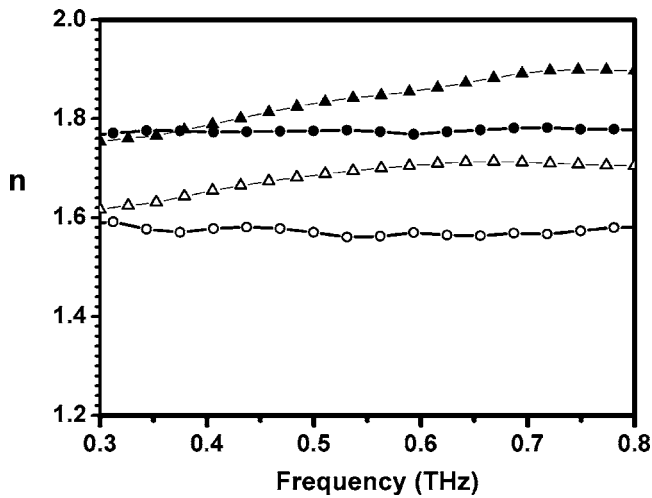


FIG. 8. Extraordinary (solid triangles) and ordinary (open triangles) refractive indices for 5CB at 25 °C reported in Ref. 19 are plotted together with the corresponding data (solid and open circles) measured as functions of frequency.

birefringence of 0.20 ± 0.02 in the same frequency range. The plausible sources of discrepancies are discussed here.

To illustrate, the two sets of data on real part of the refractive indices for 5CB at 25 °C are reproduced in Fig. 8. The discrepancy can be explained by artifacts introduced by experimental geometry and procedures. First of all, the terahertz beam is collimated in the present setup, as opposed to placement of the LC cell at the beam focus in our earlier work. The beam curvature must be taken into account for the focused beam in the Fabry–Pérot factor of Eq. (3). Previously, Duvallaret *et al.*³⁵ pointed out that an approximate calculation could lead to an erroneous trend in rising indices of refraction with frequency, if the Fabry–Pérot factor did not properly take into account. Second, we now purge the terahertz spectrometer with dry nitrogen. Note that we have set the complex refractive index of air \tilde{n}_{air} to be one in our analysis. This is an approximation that requires correction in the presence of moist air. The effect of water vapor absorption²⁸ in the beam path also manifests itself in the temporal terahertz waveform as oscillations after the main signal [see Fig. 3(a)]. This is compounded by reflective signals from the quartz-LC interfaces. These reflective signals appear about 10 ps after the main signal, while their fluctuating tails due to water vapor absorption last for another 25 ps afterward. In treating the LC sample as optically thick, one needs to remove the above reflective signals. Arbitrarily removing the undesirable peaks too close to the main peak could cut off part of the signal and render the deduced terahertz optical constants less accurate. These difficulties can be circumvented by employing substrates as thick as possible and purging the terahertz-TDS. To check, we have also conducted another set of measurements with the collimated beam geometry and room air (without purging). The results are shown in Fig. 9. A rising trend can still be discerned.

E. Error analysis

The accuracy of the measured indices has been checked by examining all the possible error sources. In our case, these

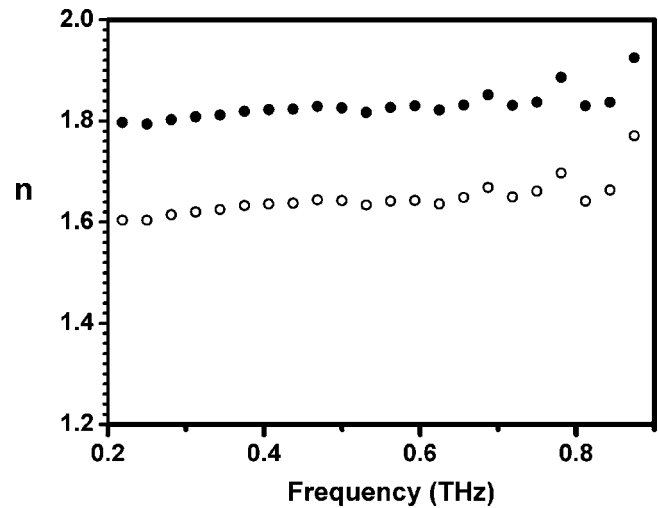


FIG. 9. Extraordinary (solid circles) and ordinary (open circles) refractive indices of 5CB measured by the terahertz time-domain spectrometer, not purged with dry nitrogen. The terahertz beam passed through the cell is collimated and at normal incidence.

include system fluctuation, calculation model, the accuracy of the thickness of the LC layer, aligned quality of the LC and the accuracy of the index of the substrates, and so on. We will discuss these one by one.

In order to check the system fluctuation and stability, we did several tests, e.g., the repeatability of the temporal signals, which include the phase and power spectra after applying FFT to it. We also measured the optical constants of well known material such as fused silica in this frequency range. For the repeatability test, we measured the temporal signals several times at a time interval of 5 min. The time-domain signals were repeatable to within <0.01 ps of each other. We also compared the phase and power spectra of the signals to each other. The ratios of the power spectra of the 2 THz signals recorded at different time need to be nearly one (>0.98). The phase fluctuation, attributed mainly to the laser noise or the instability of the optic components, was less than 5° . This is only about 1% of the predicted phase shift due to the 260- μm -thick LC cell. The measured frequency-dependent index of the 3-mm-thick fused silica substrates at room temperature is 1.951 without dispersion and absorption in the range of 0.2–1.5 THz, in good agreement with the data from literature.³⁶

It is expected that the thickness of the LC layer, the alignment quality of LC cell and the purity of LC will all affect the accuracy of the extracted optical constants. In principle, the thicker the layer is, the more accurate the results are. However, the LC layer thickness is limited by the requirement of stable LC alignment. The alignment quality of the 260- μm -thick cell was checked by looking at the order parameter determined from the measured temperature-dependent birefringence at terahertz frequencies. This shows that the alignment of our cell is as good as that in a thin sample (less than 10 μm thickness). We did not chemically analyze the purity of the 5CB (Merck) we used. The clearing point of LCs, however, correlates directly to its purity. It was found to be 34 °C in our work, consistent with what people reported for pure 5CB (34.5–35.5 °C).³⁷ The imaginary part

of the refractive index of 5CB we measured is about <0.02 , which is relatively small. The thickness of the LC layer in the experiment is $260\ \mu\text{m}$, which might not be the optimum thickness for accurate measurements. However, we can conclude that there is no resonant absorption in this frequency range as the measured real indices are spectrally flat and smooth. In order to determine accurate imaginary indices (extinction coefficient), we also measured a 2.0-mm-thick 5CB sample in isotropic phase (see Fig. 5). Results from this thick sample also suggest that there is no sharp resonance in this frequency range and the extinction coefficient of 5CB in the isotropic phase is less than 0.02 in the frequency range of 0.2–1.0 THz.

V. CONCLUSIONS

We report the frequency dependence and the temperature dependence of the optical constants of 5CB in both nematic and isotropic phases by using terahertz-TDS. We found that the extinction coefficient of 5CB is relatively small (<0.02) and without sharp absorption features in the frequency range of 0.2–1.0 THz. At $25\ ^\circ\text{C}$, the extraordinary and ordinary indices of refraction of 5CB are $n_e=1.77$ and $n_o=1.58$, giving rise to a birefringence of 0.20 ± 0.02 in the same frequency range. The order parameter extracted from temperature-dependent birefringence of 5CB agrees well with similar results in visible region.

ACKNOWLEDGMENTS

This work was supported in part by the PPAEU-II and Grant No. NSC 95-2221-E-009-249 from the National Science Council as well as the ATU program of the Ministry of Education of the Republic of China.

- ¹R. Chang, *Mater. Res. Bull.* **7**, 267 (1972); R. Chang, *Mol. Cryst. Liq. Cryst.* **30**, 155 (1975).
- ²R. A. Soref and M. J. Rafuse, *J. Appl. Phys.* **43**, 2029 (1972).
- ³W. Haase and D. Potzsch, *Mol. Cryst. Liq. Cryst.* **38**, 77 (1977).
- ⁴E. G. Hanson and Y. R. Shen, *Mol. Cryst. Liq. Cryst.* **36**, 193 (1976).
- ⁵E. Miraldi, C. Oldano, L. Trossi, and P. T. Valabrega, *Appl. Opt.* **21**, 4163 (1982).
- ⁶S. T. Wu, U. Efron, and L. V. Hess, *Appl. Phys. Lett.* **44**, 1033 (1984).
- ⁷I. C. Khoo, R. R. Michael, and G. M. Finn, *Appl. Phys. Lett.* **52**, 2108 (1988).
- ⁸P. Joffre, G. Illiaquer, and J. P. Huignard, *Proc. SPIE* **1126**, 13 (1989).
- ⁹S. T. Wu, J. D. Margerum, H. B. Meng, C. S. Hsu, and L. R. Dalton, *Appl.*

- Phys. Lett.* **64**, 1204 (1994).
- ¹⁰K. C. Lim, J. D. Margerum, A. M. Lackner, L. J. Miller, E. Sherman, and W. H. Smith, *Liq. Cryst.* **14**, 327 (1993).
- ¹¹K. C. Lim, J. D. Margerum, and A. M. Lackner, *Appl. Phys. Lett.* **62**, 1065 (1993).
- ¹²F. Guérin, J. M. Chappe, P. Joffre, and D. Dolfi, *Jpn. J. Appl. Phys., Part 1* **36**, 4409 (1997).
- ¹³M. Evans, M. Davies, and I. Larkin, *J. Chem. Soc., Faraday Trans. 1* **69**, 1011 (1973).
- ¹⁴B. J. Bulkin and W. B. Lok, *J. Phys. Chem.* **77**, 326 (1973).
- ¹⁵T. Nose, S. Sato, K. Mizuno, J. Bae, and T. Nozokido, *Appl. Opt.* **36**, 6383 (1997).
- ¹⁶D. Mittleman, *Sensing with Terahertz Radiation*, 1st ed. (Springer, New York, 2002).
- ¹⁷T.-R. Tsai, C.-Y. Chen, C.-L. Pan, R.-P. Pan, and X.-C. Zhang, *Appl. Opt.* **42**, 2372 (2003).
- ¹⁸R.-P. Pan, T.-R. Tsai, C.-Y. Chen, and C.-L. Pan, *J. Biol. Phys.* **29**, 335 (2003).
- ¹⁹R.-P. Pan, T.-R. Tsai, C.-Y. Chen, C.-H. Wang, and C.-L. Pan, *Mol. Cryst. Liq. Cryst.* **409**, 137 (2004).
- ²⁰C.-Y. Chen, C.-F. Hsieh, Y.-F. Lin, R.-P. Pan, and C.-L. Pan, *Opt. Express* **12**, 2625 (2004).
- ²¹F. Rutz, T. Hasek, M. Koch, H. Richter, and U. Ewert, *Appl. Phys. Lett.* **89**, 221911 (2006).
- ²²M. Oh-e, H. Yokoyama, M. Koeberg, E. Hendry, and M. Bonn, *Opt. Express* **14**, 11433 (2006).
- ²³J. Nishizawa, T. Yamada, T. Sasaki, T. Tanabe, T. Wadayama, T. Tanno, and K. Suto, *Appl. Surf. Sci.* **252**, 4226 (2006).
- ²⁴Y. Takanishi, K. Ishikawa, J. Watanabe, H. Takezoe, M. Yamashita, and K. Kawase, *Phys. Rev. E* **71**, 061701 (2005).
- ²⁵M. Nakamura, *J. Appl. Phys.* **52**, 4561 (1981).
- ²⁶T. J. Scheffer and J. Nehring, *J. Appl. Phys.* **48**, 1783 (1977).
- ²⁷C.-L. Pan, C.-F. Hsieh, R.-P. Pan, M. Tanaka, F. Miyamaru, M. Tani, and M. Hangyo, *Opt. Express* **13**, 30 (2005).
- ²⁸M. van Exter, Ch. Fattinger, and D. Grischkowsky, *Opt. Lett.* **14**, 1128 (1989).
- ²⁹E. Hecht, *Optics*, 3rd ed. (Addison Wesley Longman, New York, 1998), Chap. 4.
- ³⁰*Handbook of Mathematical Functions with Formulas, Graphs, and Mathematical Tables*, 9th ed., edited by M. Abramowitz and I. A. Stegun (Dover, New York, 1972).
- ³¹R. G. Horn, *J. Phys. (France)* **39**, 105 (1978).
- ³²S. Chandrasekhar, *Liquid Crystal*, 2nd ed. (Cambridge University Press, New York, 1992).
- ³³S. Brugioni, S. Faetti, and R. Meucci, *Liq. Cryst.* **30**, 927 (2003).
- ³⁴B. Bahadur, *Liquid Crystals: Applications and Uses* (World Scientific, Singapore, 1995), Vol. 1.
- ³⁵L. Duvillaret, F. Garet, and J. Coutaz, *IEEE J. Sel. Top. Quantum Electron.* **2**, 739 (1996).
- ³⁶D. Grischkowsky, S. R. Keiding, M. van Exter, and C. Fattinger, *J. Opt. Soc. Am. B* **7**, 2006 (1990).
- ³⁷I.-C. Khoo, *Liquid Crystals-Physical Properties and Nonlinear Optical Phenomena* (Wiley-Interscience, New York, 1995).